Compartmentalized Calcium Signaling in Cilia Regulates Intraflagellar Transport

Peter Collingridge[1], Colin Brownlee[1,2,*], and Glen L. Wheeler[1,3,*]
1Marine Biological Association, Citadel Hill, Plymouth PL1 2PB, UK
2Ocean and Earth Sciences, University of Southampton, Southampton SO14 3ZH, UK
3Plymouth Marine Laboratory, Prospect Place, The Hoe, Plymouth PL1 3DH, UK
*Correspondence: cbr@mba.ac.uk (C.B.), glw@pml.ac.uk (G.L.W.)

Intraflagellar transport (IFT) underpins many of the important cellular roles of cilia and flagella in signaling and motility [1–4]. The microtubule motors kinesin-2 and cytoplasmic dynein 1b drive IFT particles (protein complexes carrying ciliary component proteins) along the axoneme to facilitate the assembly and maintenance of cilia. IFT is regulated primarily by cargo loading onto the IFT particles, although evidence suggests that IFT particles also exhibit differential rates of movement [5–7]. Here we demonstrate that intraflagellar Ca^{2+} elevations act to directly regulate the movement of IFT particles. IFT-driven movement of adherent flagella membrane glycoproteins in the model alga *Chlamydomonas* enables flagella-mediated gliding motility [8–10]. We find that surface contact promotes the localized accumulation of IFT particles in *Chlamydomonas* flagella. Highly compartmentalized intraflagellar Ca^{2+} elevations initiate retrograde transport of paused IFT particles to modulate their accumulation. Gliding motility induces mechanosensitive intraflagellar Ca^{2+} elevations in trailing (dragging) flagella only, acting to specifically clear the accumulated microtubule motors from individual flagella and prevent a futile tug-of-war. Our results demonstrate that compartmentalized intraciliary Ca^{2+} signaling can regulate the movement of IFT particles and is therefore likely to play a central role in directing the movement and distribution of many ciliary proteins.

Results

Dynamic Compartmentalized Ca^{2+} Elevations in *Chlamydomonas* Flagella

Ca^{2+}-dependent signaling processes are implicated in many aspects of ciliary function [11–13], although the difficulty of visualizing ciliary Ca^{2+} in many organisms has hindered mechanistic understanding of its role, particularly in relation to sensory roles. We used total internal reflection fluorescence microscopy (TIRFM) to image gliding *Chlamydomonas* cells loaded biolistically with a Ca^{2+} indicator (Oregon green BAPTA dextran) [14] (Figure 1A; see Figures S1A and S1B available online). *Chlamydomonas* flagella exhibited frequent transient Ca^{2+} elevations that often encompassed the full flagella length (Figure 1B; Figure S1C; Movie S1). However, Ca^{2+} elevations in individual flagella were highly compartmentalized, as they did not coincide with Ca^{2+} elevations in the cytosol or the other flagellum (Figure 1B; Figure S1D). Thus, *Chlamydomonas* flagella can operate as independent Ca^{2+} signaling entities.

In gliding flagella, the retrograde movement (i.e., toward the cell body) of clusters of an adherent flagella membrane glycoprotein (FMG-1B) along the ‘‘lead’’ flagellum propels the cell body forward, dragging the ‘‘trailing’’ flagellum behind it [8, 9]. Extracellular Ca^{2+} is required for the movement of FMG-1B in the flagella membrane [9], and we found that intraflagellar Ca^{2+} elevations were associated with gliding motility. 84% of trailing flagella demonstrated a Ca^{2+} elevation either at the onset of gliding or during motility, whereas Ca^{2+} elevations were largely absent from leading flagella (Figure 1C; Figures S1E and S1F).

These results suggest that the role of Ca^{2+} signaling in gliding motility relates to sensing the dragging motion of the trailing flagellum rather than to the generation of force by the leading flagellum.

Accumulations of IFT Particles Are Associated with Gliding Motility

The intraflagellar transport (IFT) motors contribute to the movement of FMG-1B clusters in the flagella membrane [15, 16], and a recent report indicates that cytoplasmic dynein 1b acts as the gliding motor [10]. We examined the dynamics of two subunits of complex B of the IFT particle, IFT20 and IFT27 [17, 18], during gliding motility using TIRFM of fluorescently tagged proteins. We found that IFT particles accumulated at distinct locations along the length of the flagella. During gliding motility, these accumulations of IFT particles were cleared from the trailing flagellum by retrograde IFT (Figure 1D; Figure S1G; Movie S2). 91% of trailing flagella demonstrated retrograde clearance of IFT accumulations at the onset of gliding motility (n = 55), compared to 2% of leading flagella (n = 43). The accumulated IFT particles in leading flagella remained stationary relative to the substrate, suggesting that they localize to a point of contact between the flagellum and the substrate and act to propel the flagellum forward. Gliding *Chlamydomonas* cells frequently reverse direction, such that the leading flagellum becomes the trailing flagellum and vice versa. Accumulated IFT particles in leading flagella were immediately cleared via retrograde IFT as soon as the direction of travel was reversed (Figure 1D). We also found that the kinesin-associated protein (KAP), which does not show any distinct retrograde IFT [19, 20], did not exhibit the distinct accumulations or retrograde clearances demonstrated by IFT20 or IFT27 (Figure S1H). The dynamics of the accumulation and clearance of IFT particles in leading and trailing flagella are consistent with their role in providing the gliding motor [10].

Ca^{2+} Elevations Initiate Retrograde IFT of Paused IFT Particles

Ca^{2+}-dependent interactions are known to regulate the movement of microtubule motors along the cytoskeleton [21], and Ca^{2+}-dependent signaling processes may influence the velocity of anterograde IFT particles [5]. However, the spatial and temporal interactions between ciliary Ca^{2+} elevations and the movement of IFT particles have not been addressed. Simultaneous imaging of intraflagellar Ca^{2+} and IFT in *Chlamydomonas* identified a striking association between the timing of intraflagellar Ca^{2+} elevations and the retrograde clearances of accumulated IFT particles (Figures 2A and 2B). Examination of 40 flagella indicated that the initiation of retrograde transport of the paused IFT particles coincided directly with an intraflagellar Ca^{2+} elevation in each case. A statistical analysis identified a positive temporal correlation between intraflagellar Ca^{2+} and the initiation of clearances of accumulated IFT particles (Figure 2C). The entry of IFT particles into the flagellum and their turnaround at the tip do not appear to be Ca^{2+} dependent, as normal anterograde and retrograde IFT events initiate in the absence of a coinciding Ca^{2+} elevation. Intraflagellar Ca^{2+} exhibited no temporal correlation with the initiation of anterograde IFT but did show a positive correlation with the initiation of retrograde IFT events, as a proportion of these arise from paused IFT particles (Figure 2C). Flagella exhibiting multiple repetitive Ca^{2+} elevations did not accumulate IFT particles and exhibited a high frequency of retrograde IFT, whereas total retrograde IFT frequency was often reduced during periods of Ca2+ quiescence (Figures 2B, 2D, and 2E). In combination, our results suggest that retrograde IFT particles in *Chlamydomonas* originate from two sources, either from the turnaround of anterograde particles at the flagella tip or from the release of paused IFT particles that have accumulated

along the length of the flagella. The former appears to be a Ca^{2+}-independent process, whereas the latter is Ca^{2+} dependent.

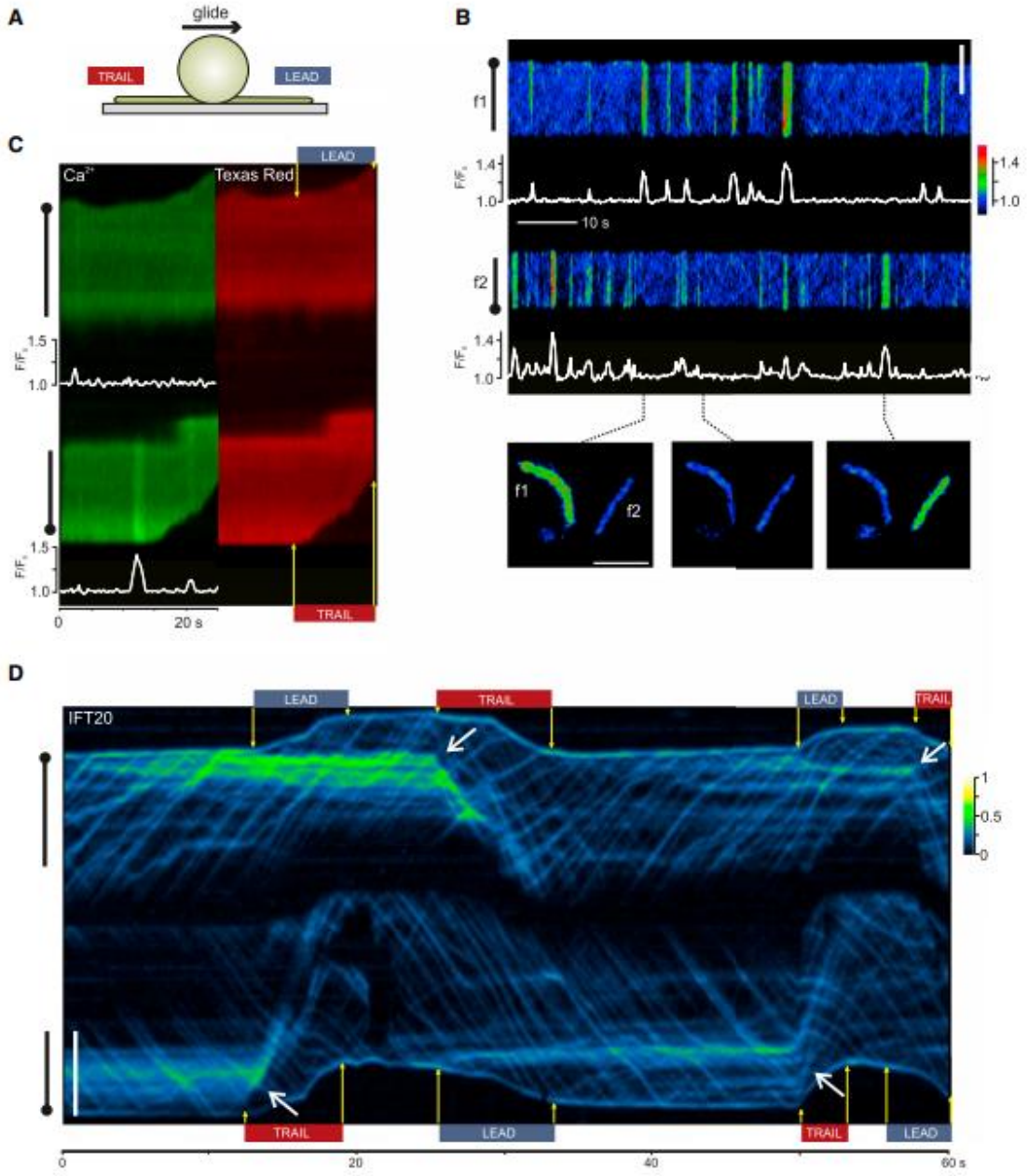

Figure 1. Ca^{2+} Signaling and Intraflagellar Transport Are Associated with Gliding Motility
(A) *Chlamydomonas* cells can adhere to and glide along a solid substrate using their flagella. Total internal reflection fluorescence microscopy (TIRFM) can be used to specifically excite fluorophores in the flagella, avoiding excitation of fluorophores in the cell body. A flagellum moving in the forward direction is termed ‘‘leading,’’ whereas movement in the reverse direction is termed ‘‘trailing.’’
(B) Independent occurrence of intraflagellar Ca^{2+} elevations. The kymograph displays spatiotemporal changes in fluorescence intensity of each *Chlamydomonas* flagella loaded with Oregon green-BAPTA dextran. A false-color image is shown to demonstrate the changes in fluorescence, with the trace below each flagellum illustrating the amplitude of Ca^{2+} elevations. Scale bar represents 5 μm.
(C) Intraflagellar Ca^{2+} elevations in gliding flagella. A representative kymograph demonstrating Ca^{2+} elevations in the trailing, but not leading, flagella coinciding with the onset of gliding motility is shown. Simultaneous imaging of a nonresponsive reference dye (Texas red) demonstrates that changes in fluorescence are not due to motion artifacts. The trace below each flagellum indicates the fluorescence ratio of Oregon green:Texas red. Scale bar represents 5 μm.

(D) Retrograde clearance of accumulated intraflagellar transport (IFT) particles coincides with gliding motility. The TIRFM kymograph demonstrates the accumulation of IFT20-mCherry in each flagellum of a gliding *Chlamydomonas* cell. At the onset of gliding motility (yellow arrows), the accumulations of IFT particles in the leading flagellum retain their position relative to the substrate but are removed from the trailing flagellum by retrograde IFT (white arrows). False color is used to illustrate the accumulation of paused IFT particles, while allowing individual moving IFT particles to be viewed (color scale indicates relative fluorescence intensity). Scale bar represents 5 µm.

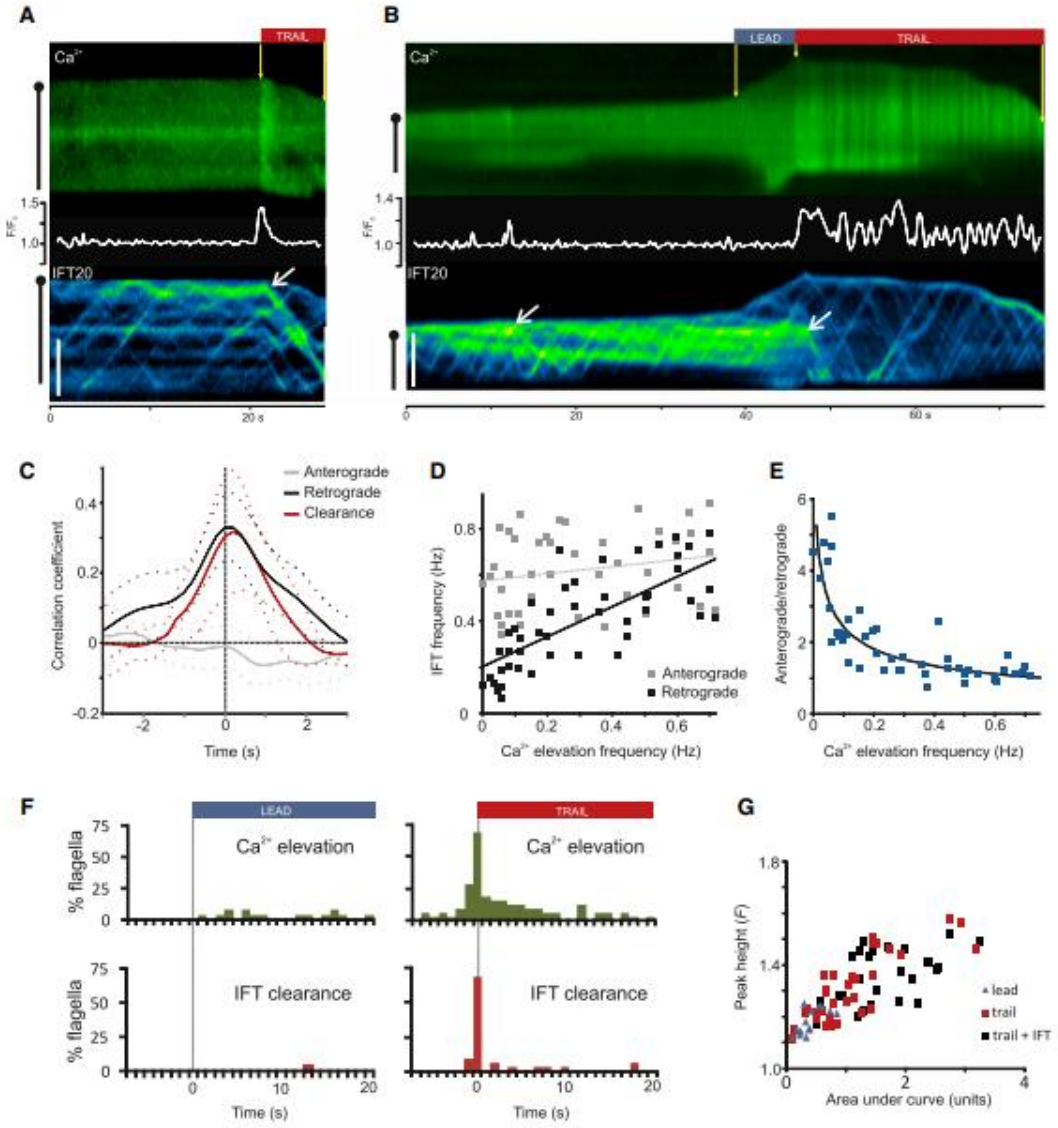

Figure 2. Ca^{2+} Signaling Regulates Retrograde IFT
(A and B) Simultaneous imaging of intraflagellar Ca^{2+} and IFT20-mCherry by TIRFM. The kymographs show that IFT20 has accumulated at several distinct locations along the flagellum. The onset of gliding motility in the trailing direction coincides with single or multiple intraflagellar Ca^{2+} elevations that coincide directly with the removal of the accumulated IFT20 by retrograde IFT (white arrows). Scale bar represents 5 µm.
(C) Mean Pearson's cross-correlation analyses show that intraflagellar Ca2+ displays a positive temporal correlation with the initiation of retrograde events (n = 8 flagella), but not with anterograde events (n = 7). Specific analysis of retrograde clearances of accumulated IFT particles also displays a positive correlation with intraflagellar Ca2+ (n = 7). Dotted lines represent 95% confidence intervals.
(D) Frequency of anterograde and retrograde transport of IFT20 as a function of the frequency of intraflagellar Ca^{2+} elevations. There is a positive correlation between the frequency of intraflagellar Ca^{2+} elevations and retrograde IFT (R2 = 0.55, solid line), but not anterograde IFT (R2 = 0.04, dashed line). n = 46.
(E) Ratio of the frequency of anterograde/retrograde IFT in individual flagella relative to the frequency of intraflagellar Ca^{2+} elevations.
(F) Simultaneous imaging of Ca^{2+} and IFT20-mCherry in gliding cells. Frequency histograms indicate the proportion of flagella demonstrating a Ca^{2+} elevation or retrograde clearance of accumulated IFT20 at each time

point (bin = 1 s). Trailing flagella exhibit an increased incidence of Ca^{2+} elevations and clearance of accumulated IFT20, and in many cases, these events coincide with the onset of motility. There are very few Ca^{2+} elevations or IFT20 clearances in leading flagella. Leading n = 23, trailing n = 32.
(G) Characteristics of Ca^{2+} elevations in gliding flagella displayed as the maximal amplitude against the area under the curve (a measure of the total exposure to elevated Ca^{2+}).

Ca^{2+}-Dependent Regulation of IFT during Gliding

The onset of gliding motility in trailing flagella was associated with single or multiple Ca^{2+} elevations, resulting in the clearance of the accumulated IFT particles by retrograde IFT (Figure 2F). 84% of trailing flagella exhibited an intraflagellar Ca^{2+} elevation within 2 s of the onset of gliding motility, and 78% of trailing flagella exhibited a retrograde clearance of accumulated IFT20 within this period (n = 32). Each retrograde clearance corresponded to an intraflagellar Ca^{2+} elevation. 69% of trailing flagella exhibited additional Ca^{2+} elevations throughout the gliding movement. In contrast, only 4% of leading flagella exhibited a Ca^{2+} elevation within 2 s of the onset of motility, and none exhibited a retrograde clearance of accumulated IFT20 within this period (n = 23). Ca^{2+} elevations in trailing flagella exhibited a much greater mean maximal amplitude and duration than those occasionally observed in leading flagella, particularly for those Ca^{2+} elevations associated with the retrograde clearance of IFT particles, suggesting that a threshold intraflagellar Ca^{2+} concentration may be required to initiate retrograde IFT of paused IFT particles (Figure 2G; Figure S2).

The Requirement for Ca2+ Signaling in Modulating IFT Accumulation

We perfused *Chlamydomonas* cells with a Ca^{2+}-free buffer to prevent Ca^{2+} influx across the flagella membrane and inhibit Ca^{2+} signaling. The absence of external Ca^{2+} resulted in the rapid cessation of intraflagellar Ca^{2+} elevations and a dramatic accumulation of IFT20 and IFT27 in the flagella within several minutes (Figure 3A; Figure S3A). KAP-GFP did not accumulate (Figure S3B). In the initial period (0–5 min) following Ca^{2+} removal, 70% of flagella exhibited a forward glide of up to one flagella length, but only 14% of flagella demonstrated any movement in the trailing direction (n = 77). These trailing flagella did not exhibit Ca^{2+} elevations or retrograde clearances of IFT particles, with the majority of paused IFT particles remaining stationary relative to the substrate during the glide (n = 13) (Figure 3B). After 5 min in Ca^{2+}-free buffer, there was a complete inhibition of gliding motility, corresponding with the significant accumulation of IFT particles (n = 332).

The inhibition of intraflagellar Ca^{2+} elevations resulted in a decrease in the frequency of retrograde IFT, followed by a less pronounced decrease in the frequency of anterograde IFT (Figures S3C and S3D). Since we observed no direct effect of Ca^{2+} elevations on anterograde IFT, the inhibition of anterograde IFT in the absence of Ca^{2+} may result from the physical barrier presented by accumulated IFT particles or a reduction in the cytoplasmic pool of IFT particles due to reduced retrograde transport. Although the normal progression of IFT does not appear to be linked to Ca^{2+} transients, the inability to remove paused IFT particles in the absence of Ca^{2+} may result in their accumulation to an extent where progression of all IFT particles is disrupted.

IFT accumulations associated with Ca^{2+} removal were entirely restricted to those regions of the flagellum in contact with the substrate (Figure 3C; Movies S3 and S4). 85% of gliding cells exhibited a pronounced accumulation of IFT particles in regions of surface contact following Ca^{2+} removal (n = 54). In the presence of external Ca^{2+}, surface contact resulted in

a significant accumulation of IFT particles in 8.1% of gliding cells, although the majority of flagella exhibited a punctate distribution of IFT particles (n = 74).

Rapid addition of Ca^{2+} to the media was used to induce intraflagellar Ca^{2+} elevations in *Chlamydomonas* cells deprived of external Ca^{2+} [14]. No gliding motility or retrograde clearances of accumulated IFT were observed in the 1 min period preceding Ca^{2+} addition (n = 68). Following the addition of 2.5 mM Ca^{2+}, 54% of flagella exhibited an IFT clearance within 10 s, rising to 82% within a 40 s period. Simultaneous imaging of Ca^{2+} and IFT20-mCherry showed that the intraflagellar Ca^{2+} elevations generated in this manner coincided precisely with the retrograde clearance of accumulated IFT (n = 17) (Figure 3D).

Evidence for Mechanosensitive Ca^{2+} Signaling

Chlamydomonas flagella are mechanosensitive and contain several candidate mechanosensitive TRP channels [22–24]. Using a micromanipulator and a suction pipette to hold and move the cell body, we induced flagella movements along the substrate that mimicked the magnitude and velocity of gliding motility. Small movements of the cell body (<1 μm) consistently elicited intraflagellar Ca^{2+} elevations and triggered retrograde clearance of accumulated IFT particles in trailing flagella but did not result in Ca^{2+} elevations or IFT clearances in leading flagella (n = 11 cells) (Figure 4A). In the absence of external Ca^{2+}, mechanical stimulation of flagella did not result in any intraflagellar Ca^{2+} elevations or clearances of accumulated IFT particles (n = 11 cells) (Figure 4A). Inhibitors of stretch-activated channels strongly reduced the frequency of both intraflagellar Ca^{2+} elevations and IFT and inhibited gliding in a manner similar to the removal of Ca^{2+} (Figures 4B and 4C).

The Role of Flagella Membrane Potential

The simultaneous elevation of intraflagellar Ca^{2+} along the whole length of the flagellum could be mediated by changes in membrane potential resulting in the activation of voltagegated Ca^{2+} channels. Using the voltage-sensitive dye Annine-6plus [25, 26], we were able to detect transient membrane depolarization events associated with the onset of gliding motility (mean duration 0.25 s 6 0.03 SE, mean max amplitude 211.8% DF 6 0.6 SE, n = 42) that shared many similar characteristics with Ca^{2+} elevations (Figure 4D; Figure S4A). However, in contrast to Ca^{2+} elevations, changes in membrane potential in trailing flagella were closely mirrored in leading flagella, with over 90% of membrane depolarization events occurring simultaneously in both flagella (n = 42 events) (Figures S4B and S4C). Membrane depolarization events were not observed in the absence of external Ca^{2+}, indicating a requirement for Ca^{2+} influx. As Ca^{2+} elevations occur independently in each flagellum but depolarization events occur simultaneously, membrane depolarization alone cannot be responsible for inducing intraflagellar Ca^{2+} elevations. Thus, signaling during gliding is distinct from the photoshock response in swimming *Chlamydomonas* cells, in which channelrhodopsin-mediated depolarization of the whole cell activates voltage-gated Ca^{2+} channels simultaneously in both flagella [27, 28]. We cannot discount a role for depolarization-activated Ca^{2+} channels in propagating intraflagellar Ca^{2+} elevations during gliding, although specific mechanisms involving recovery from inactivation or modulation of their voltage-gating properties (such as mechanosensitive modulation) [29, 30] must exist to restrict their activity to individual flagella.

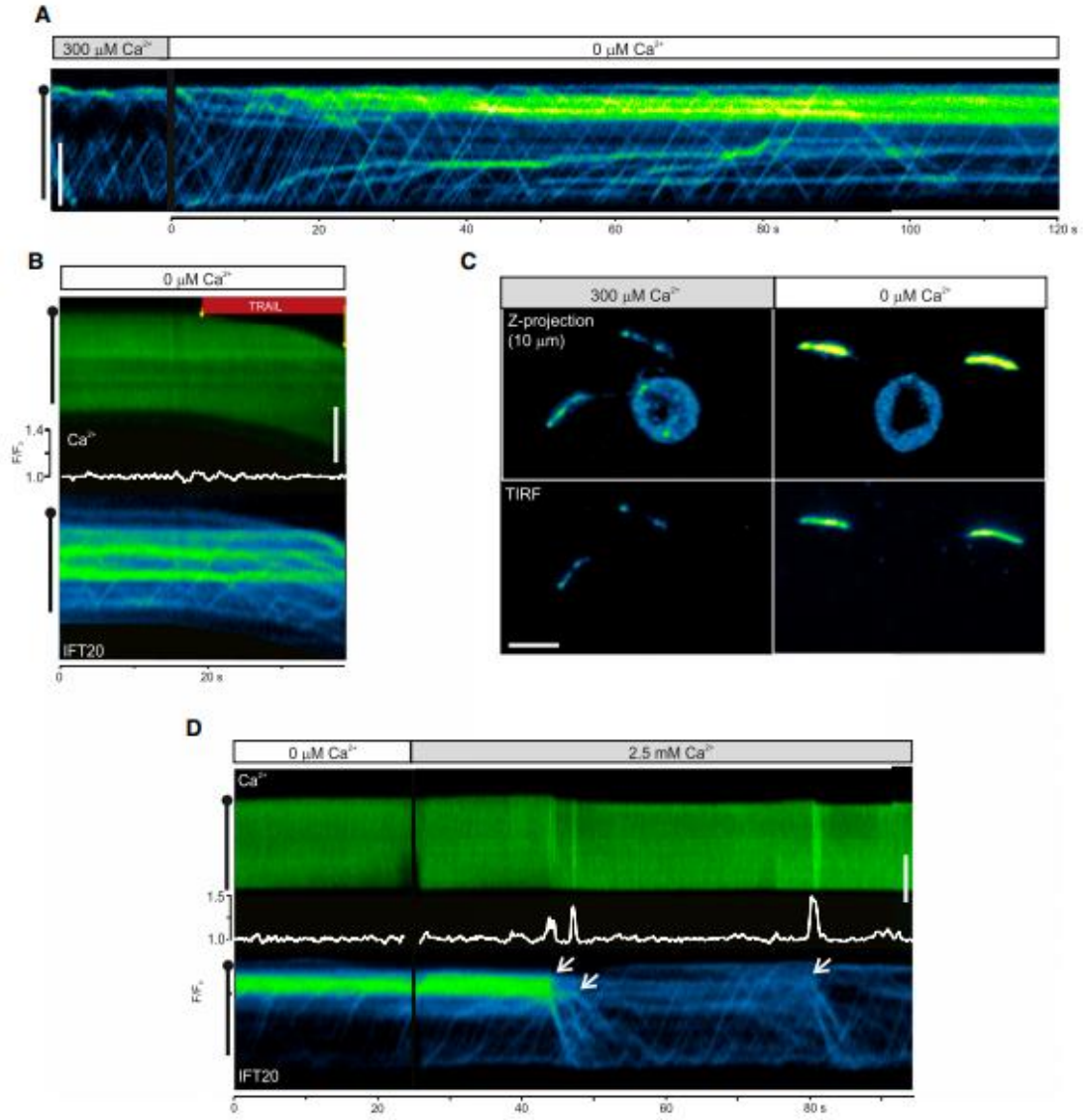

Figure 3. IFT Particles Accumulate in the Absence of External Ca2+
(A) IFT20-mCherry accumulates in flagella following removal of external Ca2+. Cells were perfused with Ca2+-free buffer containing 5 mM EGTA to prevent intraflagellar Ca2+ elevations. There is a clear and rapid accumulation of IFT particles, and both the frequency and velocity of moving IFT particles is reduced. Scale bar represents 5 µm.
(B) Trailing flagella moving in the initial period following removal of external Ca2+. No intraflagellar Ca2+ elevations or retrograde clearances of accumulated IFT were associated with gliding motility, and the majority of the accumulated IFT particles in trailing flagella remain stationary relative to the substrate. Scale bar represents 5 µm.
(C) Localization of IFT particle accumulation. Cells expressing IFT20-mCherry were resuspended in Ca2+-free buffer (200 µM EGTA) and imaged by TIRF and wide-field epifluorescence microscopy. z projections (10 µm depth, 0.4 µm slice) were created using image deconvolution. The fluorescence relating to the significant accumulations of IFT20 is almost entirely restricted to regions of surface contact, as determined by TIRF microscopy. Chlorophyll autofluorescence can be viewed in the cell body. In the presence of external Ca2+, IFT20 displays a more punctate distribution throughout the flagellum. Scale bar represents 5 µm.
(D) External Ca2+ is required to restore normal IFT. Rapid replacement of Ca2+-free buffer (200 µM EGTA) with 2.5 mM free Ca2+ induced intraflagellar Ca2+ elevations in flagella of IFT20-mCherry cells that coincide directly with the retrograde clearance of accumulated IFT (white arrows). The kymograph is representative of 17 cells. Scale bar represents 5 µm.

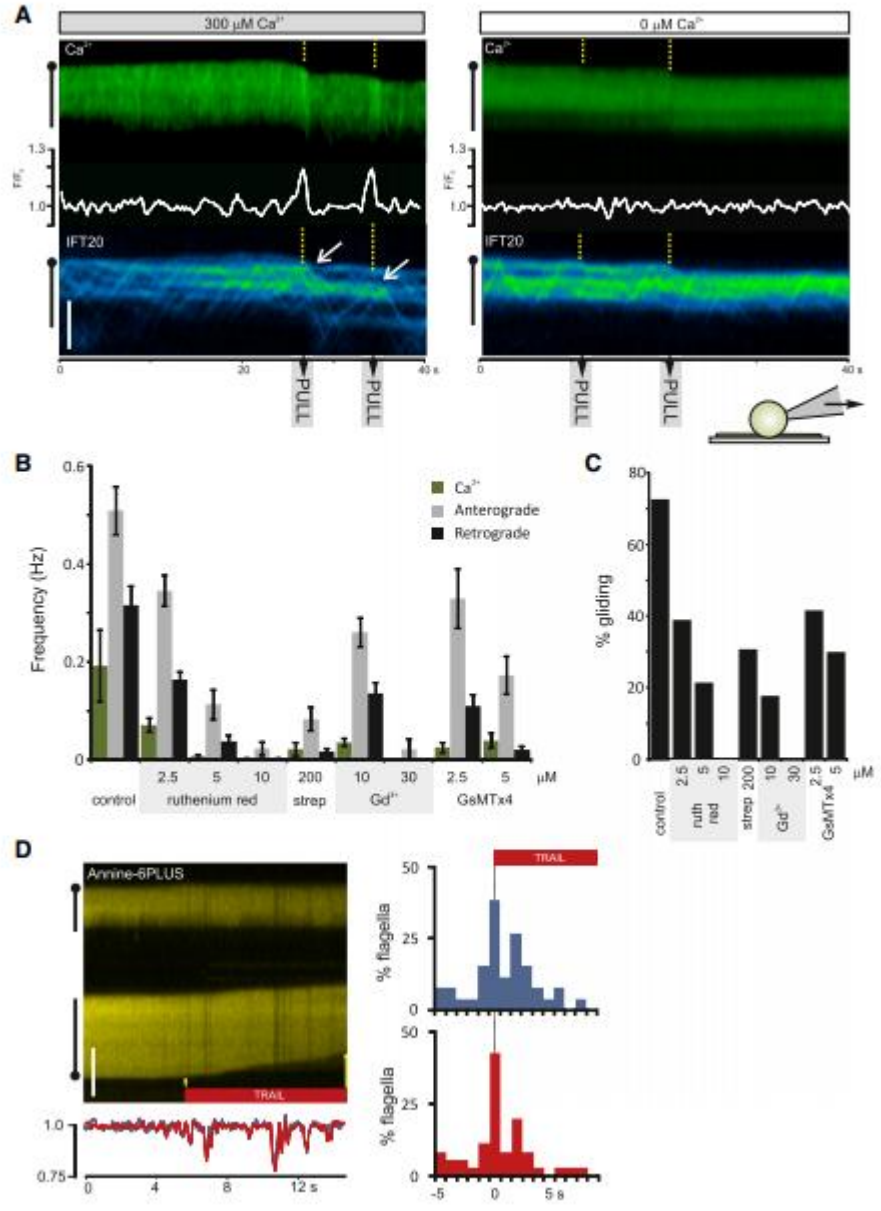

Figure 4. Evidence for Mechanosensitive Ca2+ Signaling
(A) Micromanipulation of cells to induce flagella movements. The kymographs demonstrate intraflagellar Ca2+ and movements of IFT20-mCherry following incremental movements of the cell body (highlighted in gray) to induce small gliding movements in the flagella. A suction pipette was used to hold the cell body (inset). In the presence of 300 µM free Ca2+, induced flagella movements resulted in a Ca2+ elevation and retrograde clearance of accumulated IFT20. In the absence of external Ca2+, no intraflagellar Ca2+ elevations or retrograde clearance of accumulated IFT20 were observed. Scale bar 5 represents µm.
(B) Mechanosensitive ion channel blockers inhibit intraflagellar Ca2+ elevations and IFT. The graph displays the mean frequency (6SEM) of intraflagellar Ca2+ elevations, anterograde IFT, and retrograde IFT in *Chlamydomonas* flagella (IFT20-mCherry) following the addition of ruthenium red, streptomycin, Gd3+, or GsMTx4 (n = 11–18).
(C) The percentage of cells from the experiment described in (B) exhibiting significant gliding motility (>1 µm) within a 1 min period.
(D) TIRFM of the voltage-sensitive dye Annine6plus in flagella during gliding. A decrease in fluorescence indicates depolarization of the flagella membrane potential (Figure S4). Simultaneous transient depolarization events occur in both flagella following the onset of gliding motility. Scale bar represents 5 µm. Frequency histograms are shown, demonstrating the timing of membrane depolarization events in the trailing (red) and leading (blue) flagellum at the onset of the gliding motility. Leading n = 26, trailing n = 34.

Discussion

Our findings are consistent with a requirement for Ca^{2+} -dependent regulation of IFT during flagella-mediated gliding motility and allow us to propose a mechanistic model for this process. It is likely that surface contact promotes an interaction between FMG-1B and the IFT particle, causing IFT particles to accumulate at this location. The continued accumulation of retrograde motors tethered to the substrate via the flagella membrane will eventually provide sufficient force to pull the flagellum forward. As gliding *Chlamydomonas* cells possess two flagella that pull in opposite directions, it appears that a mechanosensor, such as a stretch-activated ion channel, responds to mechanical stimuli relating to the dragging of a trailing flagellum and triggers the generation of intraflagellar Ca^{2+} elevations that are restricted to this flagellum only. The Ca^{2+} elevation acts to disrupt the interaction between the IFT particle and the flagella membrane and results in the rapid retrograde clearance of any accumulated IFT particles. The compartmentalized nature of the flagella Ca^{2+} elevations allows independent regulation of IFT in individual flagella to prevent a futile tug-of-war.

Mechanosensory Ca^{2+} signaling plays a role in both motile and nonmotile cilia, with mechanosensitive transient receptor potential (TRP) channels often acting as the mechanosensor [22, 31, 32]. Although flagella Ca^{2+} elevations were sensitive to a range of potential blockers of mechanosensitive ion channels, the exact nature of the mechanosensor in adherent *Chlamydomonas* flagella remains unclear. We find that intraflagellar Ca^{2+} elevations generated by mechanical stimuli can be highly compartmentalized, without propagation to the cytosol or to neighboring flagella. This suggests that Ca^{2+} diffusion from the cilia into the cytosol is likely to be limited, although ciliary Ca^{2+} elevations could activate Ca^{2+}-sensitive elements located at the base of the cilium or may release other second messengers that can diffuse freely into the cytosol. Our results also indicate that cilia could relay sensory information to the cell via retrograde IFT or changes in membrane potential.

IFT plays a central role in many ciliary signaling processes. For example, IFT is required for the ciliary localization of receptor proteins involved in the Hedgehog (Hh) signaling pathway, with mutants defective in IFT showing impaired signal transduction [33–35]. A direct signaling role for IFT has been demonstrated in the mating response of *Chlamydomonas*, where IFT is required for the activation of a cAMP-dependent signaling cascade resulting in gamete fusion [4]. In addition to our results, roles for second messengers in regulating IFT have been observed in the remodeling of AWB sensory cilia in C. elegans or in the control of ciliary length in mammalian cells [5, 36]. As ciliary Ca^{2+} signaling appears to be highly compartmentalized, it will be important to understand more fully the spatial and temporal dynamics of these second messengers in order to determine their mode of action on IFT.

Our findings illustrate clearly that the movement of IFT particles is highly regulated. In *Chlamydomonas*, a constant frequency of anterograde IFT is required for flagella assembly and maintenance of flagella length, whereas mutants defective in retrograde IFT are able to maintain full-length flagella for several hours [37]. Thus, retrograde IFT may be used more flexibly than anterograde IFT to perform additional functions such as gliding or signaling, so long as sufficient retrograde IFT occurs to prevent depletion of the cytoplasmic pool of IFT precursors. Prolonged or severe disruption of flagella Ca^{2+} signaling may, however, inhibit IFT sufficiently to disrupt flagella assembly. Given that Ca^{2+} signaling is central to signal transduction in cilia and IFT is highly conserved from algae to animals, it is likely that Ca^{2+}-dependent regulation of IFT plays an important role in many aspects of ciliary function.

Supplemental Information

Supplemental Information includes four figures, Supplemental Experimental Procedures, and four movies can be found with this article online at http://dx.doi.org/10.1016/j.cub.2013.09.059.

Acknowledgments

We thank Karl Lechtreck and Joel Rosenbaum for donation of *Chlamydomonas* strains and antibodies and Abdul Chrachri for assistance with electrophysiology. This work was funded by the Biotechnology and Biological Sciences Research Council UK (grant number BB/H013814/1).

References

1. Singla, V., and Reiter, J.F. (2006). The primary cilium as the cell's antenna: signaling at a sensory organelle. Science 313, 629–633.

2. Christensen, S.T., Pedersen, L.B., Schneider, L., and Satir, P. (2007). Sensory cilia and integration of signal transduction in human health and disease. Traffic 8, 97–109.

3. Huangfu, D., Liu, A., Rakeman, A.S., Murcia, N.S., Niswander, L., and Anderson, K.V. (2003). Hedgehog signalling in the mouse requires intraflagellar transport proteins. Nature 426, 83–87.

4. Wang, Q., Pan, J., and Snell, W.J. (2006). Intraflagellar transport particles participate directly in cilium-generated signaling in *Chlamydomonas*. Cell 125, 549–562.

5. Besschetnova, T.Y., Kolpakova-Hart, E., Guan, Y., Zhou, J., Olsen, B.R., and Shah, J.V. (2010). Identification of signaling pathways regulating primary cilium length and flow-mediated adaptation. Curr. Biol. 20, 182–187.

6. Buisson, J., Chenouard, N., Lagache, T., Blisnick, T., Olivo-Marin, J.C., and Bastin, P. (2013). Intraflagellar transport proteins cycle between the flagellum and its base. J. Cell Sci. 126, 327–338.

7. Dentler, W. (2005). Intraflagellar transport (IFT) during assembly and disassembly of *Chlamydomonas* flagella. J. Cell Biol. 170, 649–659.

8. Bloodgood, R.A. (1981). Flagella-dependent gliding motility in *Chlamydomonas*. Protoplasma 106, 183–192.

9. Bloodgood, R.A., and Salomonsky, N.L. (1990). Calcium influx regulates antibody-induced glycoprotein movements within the *Chlamydomonas* flagellar membrane. J. Cell Sci. 96, 27–33.

10. Shih, S.M., Engel, B.D., Kocabas, F., Bilyard, T., Gennerich, A., Marshall, W.F., and Yildiz, A. (2013). Intraflagellar transport drives flagellar surface motility. Elife 2, e00744.

11. Kamiya, R., and Witman, G.B. (1984). Submicromolar levels of calcium control the balance of beating between the 2 flagella in demembranated models of *Chlamydomonas*. J. Cell. Biol. 98, 97–107.

12. Lefebvre, P.A., Nordstrom, S.A., Moulder, J.E., and Rosenbaum, J.L. (1978). Flagellar elongation and shortening in *Chlamydomonas*. IV. Effects of flagellar detachment, regeneration, and resorption on the induction of flagellar protein synthesis. J. Cell Biol. 78, 8–27.

13. Wood, C.D., Nishigaki, T., Furuta, T., Baba, S.A., and Darszon, A. (2005). Real-time analysis of the role of Ca2+ in flagellar movement and motility in single sea urchin sperm. J. Cell Biol. 169, 725–731.

14. Wheeler, G.L., Joint, I., and Brownlee, C. (2008). Rapid spatiotemporal patterning of cytosolic Ca2+ underlies flagellar excision in *Chlamydomonas* reinhardtii. Plant J. 53, 401–413.

15. Kozminski, K.G., Beech, P.L., and Rosenbaum, J.L. (1995). The *Chlamydomonas* kinesin-like protein FLA10 is involved in motility associated with the flagellar membrane. J. Cell Biol. 131, 1517–1527.

16. Laib, J.A., Marin, J.A., Bloodgood, R.A., and Guilford, W.H. (2009). The reciprocal coordination and mechanics of molecular motors in living cells. Proc. Natl. Acad. Sci. USA 106, 3190–3195.

17. Lechtreck, K.F., Johnson, E.C., Sakai, T., Cochran, D., Ballif, B.A., Rush, J., Pazour, G.J., Ikebe, M., and Witman, G.B. (2009). The *Chlamydomonas* reinhardtii BBSome is an IFT cargo required for export of specific signaling proteins from flagella. J. Cell Biol. 187, 1117–1132.

18. Qin, H., Wang, Z., Diener, D., and Rosenbaum, J. (2007). Intraflagellar transport protein 27 is a small G protein involved in cell-cycle control. Curr. Biol. 17, 193–202.

19. Engel, B.D., Ludington, W.B., and Marshall, W.F. (2009). Intraflagellar transport particle size scales inversely with flagellar length: revisiting the balance-point length control model. J. Cell Biol. 187, 81–89.

20. Mueller, J., Perrone, C.A., Bower, R., Cole, D.G., and Porter, M.E. (2005). The FLA3 KAP subunit is required for localization of kinesin-2 to the site of flagellar assembly and processive anterograde intraflagellar transport. Mol. Biol. Cell 16, 1341–1354.

21. Wang, X., and Schwarz, T.L. (2009). The mechanism of Ca2+-dependent regulation of kinesin-mediated mitochondrial motility. Cell 136, 163–174.

22. Fujiu, K., Nakayama, Y., Iida, H., Sokabe, M., and Yoshimura, K. (2011). Mechanoreception in motile flagella of *Chlamydomonas*. Nat. Cell Biol. 13, 630–632.

23. Huang, K., Diener, D.R., Mitchell, A., Pazour, G.J., Witman, G.B., and Rosenbaum, J.L. (2007). Function and dynamics of PKD2 in *Chlamydomonas* reinhardtii flagella. J. Cell Biol. 179, 501–514.

24. Yoshimura, K. (1996). A novel type of mechanoreception by the flagella of *Chlamydomonas*. J. Exp. Biol. 199, 295–302.

25. Fromherz, P., Hu¨ bener, G., Kuhn, B., and Hinner, M.J. (2008). ANNINE6plus, a voltage-sensitive dye with good solubility, strong membrane binding and high sensitivity. Eur. Biophys. J. 37, 509–514.

26. Page` s, S., Coˆ te´ , D., and De Koninck, P. (2011). Optophysiological approach to resolve neuronal action potentials with high spatial and temporal resolution in cultured neurons. Front. Cell Neurosci. 5, 20.

27. Fujiu, K., Nakayama, Y., Yanagisawa, A., Sokabe, M., and Yoshimura, K. (2009). *Chlamydomonas* CAV2 encodes a voltage- dependent calcium channel required for the flagellar waveform conversion. Curr. Biol. 19, 133–139.

28. Holland, E.M., Harz, H., Uhl, R., and Hegemann, P. (1997). Control of phobic behavioral responses by rhodopsin-induced photocurrents in *Chlamydomonas*. Biophys. J. 73, 1395–1401.

29. Calabrese, B., Tabarean, I.V., Juranka, P., and Morris, C.E. (2002). Mechanosensitivity of N-type calcium channel currents. Biophys. J. 83, 2560–2574.

30. Stru¨ nker, T., Weyand, I., Bo¨ nigk, W., Van, Q., Loogen, A., Brown, J.E., Kashikar, N., Hagen, V., Krause, E., and Kaupp, U.B. (2006). A K+ -selective cGMP-gated ion channel controls chemosensation of sperm. Nat. Cell Biol. 8, 1149–1154.

31. Yoshiba, S., Shiratori, H., Kuo, I.Y., Kawasumi, A., Shinohara, K., Nonaka, S., Asai, Y., Sasaki, G., Belo, J.A., Sasaki, H., et al. (2012). Cilia at the node of mouse embryos sense fluid flow for left-right determination via Pkd2. Science 338, 226–231.

32. Gong, Z., Son, W., Chung, Y.D., Kim, J., Shin, D.W., McClung, C.A., Lee, Y., Lee, H.W., Chang, D.J., Kaang, B.K., et al. (2004). Two interdependent TRPV channel subunits, inactive and Nanchung, mediate hearing in Drosophila. J. Neurosci. 24, 9059–9066.

33. Mukhopadhyay, S., Wen, X., Ratti, N., Loktev, A., Rangell, L., Scales, S.J., and Jackson, P.K. (2013). The ciliary G-protein-coupled receptor Gpr161 negatively regulates the Sonic hedgehog pathway via cAMP signaling. Cell 152, 210–223.

34. Qin, J., Lin, Y., Norman, R.X., Ko, H.W., and Eggenschwiler, J.T. (2011). Intraflagellar transport protein 122 antagonizes Sonic Hedgehog signaling and controls ciliary localization of pathway components. Proc. Natl. Acad. Sci. USA 108, 1456–1461.

35. Tran, P.V., Haycraft, C.J., Besschetnova, T.Y., Turbe-Doan, A., Stottmann, R.W., Herron, B.J., Chesebro, A.L., Qiu, H., Scherz, P.J., Shah, J.V., et al. (2008). THM1 negatively modulates mouse sonic hedgehog signal transduction and affects retrograde intraflagellar transport in cilia. Nat. Genet. 40, 403–410.

36. Mukhopadhyay, S., Lu, Y., Shaham, S., and Sengupta, P. (2008). Sensory signaling-dependent remodeling of olfactory cilia architecture in C. elegans. Dev. Cell 14, 762–774.

37. Engel, B.D., Ishikawa, H., Wemmer, K.A., Geimer, S., Wakabayashi, K., Hirono, M., Craige, B., Pazour, G.J., Witman, G.B., Kamiya, R., and Marshall, W.F. (2012). The role of retrograde intraflagellar transport in flagellar assembly, maintenance, and function. J. Cell Biol. 199, 151–167.